

Dynamics of Phases in a Standpipe

S.L. Soo¹ and C. Zhu²

A standpipe, in combination with a cyclone and venturi, can replace storage bins for research and testing in gas-solid flow and pneumatic transport in a recycling pipe flow system with minimum investment of solids or size of test sample and for unlimited test durations. Satisfactory operation of such a system, however, depends on minimal leakage flow up the standpipe. The favorable pressure gradient in the particle phase due to gravity and phase-interactions may overcome the effect of pressure of the return air stream which is higher than that at the top of the standpipe. The meaning of pressure of the particle phase due to static head and kinetics of motion is discussed. Design criteria are demonstrated through basic relations and by experimental results.

INTRODUCTION

For continuous testing of pipe flow of a dense suspension, a test loop with a cyclone-standpipe-tee configuration, Figure 1, for the separation and reintroduction of particles has been used [1]. The basic design takes advantage of the nature of a standpipe [2,3] (both consist of the career research of L.S. Leung). This 51 mm (2 in) diameter pipe flow loop, with an investment of 10 kg of solid particles for continuous testing, replaces a bin-system with 2 one-ton bins for 30 minutes test duration at a mass flow ratio of solid to air of up to 12 at an air velocity of 20 m/s, or 2 ton/hr solid flow rate. Satisfactory operation of the cyclone-standpipe system depends on a negligible leakage flow up the standpipe. Depending on the magnitude of interacting parameters, the down flow of solids may induce a downward flow of air. However, a large rate of solid feed and large pipe line flow velocity may lead to upward flow of air in

the standpipe and instability of solid feed with bubble formation.

BASIC RELATIONS

The standpipe with its ball valve is shown in Figure 2, together with the notations for the pressures along its height. P_{s1} is the pressure above the bed of solid particles, P_{s2} is that at the inlet of the ball valve and P_{s3} is that at its outlet. P_{s2} includes the hydrostatic head of the solid bed. What constitutes the pressure of the solid phase has been a topic of interest [4,5]. In the transition from a packed bed to fluidization in a standpipe, the momentum equation of a phase k can be represented as [6]:

$$\begin{aligned} & \alpha_k \rho_k (\partial U_{ki} / \partial t) + \alpha_k \rho_k U_{kj} (\partial U_{ki} / \partial x_j) \\ & = -(\partial P_k / \partial x_i) + (\partial / \partial x_j) (\tau_{ij} + \tau_{ij}^T) \\ & + \alpha_k \rho_k f_j + \alpha_k \rho_k F_{ki} (U_{li} - U_{ki}), \end{aligned} \quad (1)$$

1. Dept. of Mechanical and Industrial Engineering, University of Illinois at Urbana-Champaign, Urbana, IL, USA 61801.

2. Dept. of Chemical Engineering, Ohio State University, Columbus, OH USA 43210.

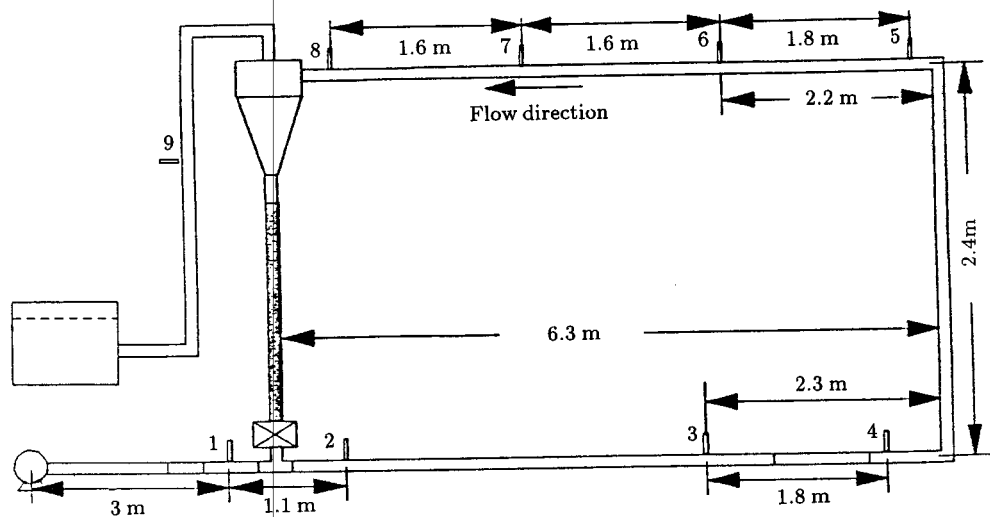


Figure 1. 51 mm diameter test loop and locations of pressure sensors.

where ρ_k is the density of phase k ; α_k , its volume fraction; U_{ki} , its i -th component of mean velocity; t is the time; x_j , j -th coordinate; P_k is the pressure of phase k ; τ_{ij} , the i -th component of stress in the j -th plane; T_{ij}^T , the Reynolds stress due to turbulence; f_i is the field force per unit mass; F_{kl} is the relaxation time constant of phase k as influenced by another phase l . For a system of phases p for particles and f for the gas, and for

nearly fully developed motion, the momentum equation of the particle phase becomes (p corresponds to k , g to l in Equation 1): ($p \dots 1$)

$$\begin{aligned} (dP_p/dz) = & (d/dr)r\mu_{pp}(dW_p/dr) \\ & + (\partial/\partial z)(\alpha_p\rho_p \langle u_p u_p \rangle) \\ & + \alpha_p\rho_p g + \alpha_p\rho_p F_{pf}(W_f - W_p), \end{aligned} \quad (2)$$

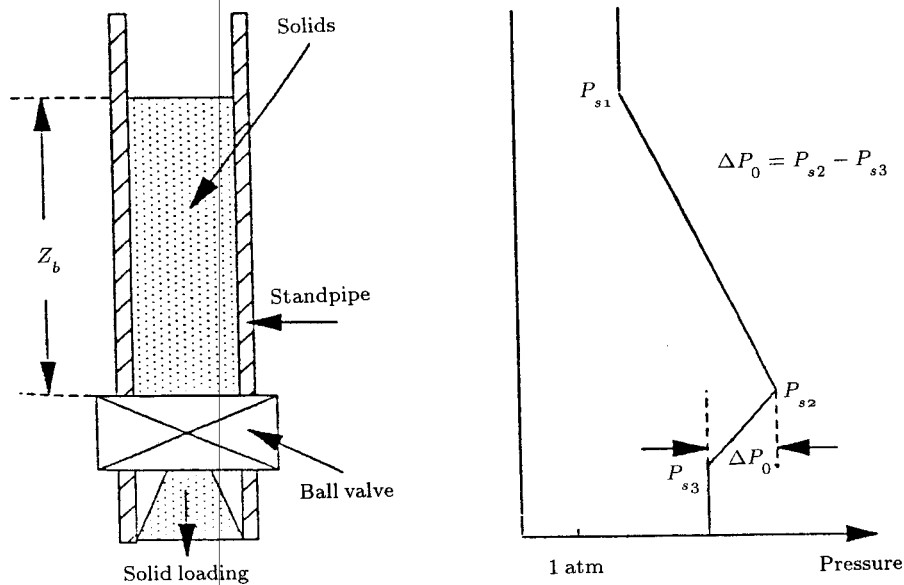


Figure 2. Schematic of standpipe and notations of air pressure distribution.

where the axial coordinate z , conjugate average velocity W , and gravitational acceleration g all point downward as positive; r is the radial coordinate; μ_{pp} is the viscosity of particle phase due to particle-particle interaction [6]; $\langle u_p u_p \rangle$ in this case is the mean squared random velocity in the radial direction constituting the Reynolds stress with particle cloud density $\alpha_p \rho_p$; F_{pf} is the relaxation time constant due to fluid particle interaction. F_{pf} is given by [7, or see 6]:

$$\begin{aligned} F_{pf} &= [75\alpha_p\mu/2(1-\alpha_p)^2\rho_p a^2] \\ &+ [1.75\rho_f |W_p - W_f| / 2(1-\alpha_p)\rho_p a] \\ &\equiv [A_1 + A_2 |W_p - W_f|] / \alpha_p \rho_p \end{aligned} \quad (3)$$

where μ is the viscosity of the fluid; a is the radius of the particles; the second term on the RHS accounts for the inertia effect. We note that in Equation 2, the first term on the r.h.s. is small in packed bed flow, the rest of the terms correspond to what is referred to as the particle pressure in [4] and [5]. This random velocity in a fluidized bed of 1 mm glass particles measured by [8] was nearly 10% of the superficial gas velocity, giving a rate of momentum transfer at the wall of less than 10 Pa. Even with the increased random velocity and decrease in concentration of particles at the increased elevation, there is insufficient change in Reynolds stress in the form of collision on the wall strain gauge by random motion of particles to give the pressure drop measured by [4]. Since the average velocity $W_p = 0$ in a packed and fluidized bed, and W_f is upward and negative (particles are lifted by the gas when fluidization occurs), reducing the gravity effect, the wall strain gauge of [4] sensed the combined effects in Equation 2. Therefore, the particle pressure was not just due to collision of particles on the wall. The measured particle pressure therefore does not change the basic relations of multiphase flow.

FLOW OF PHASES

Relations concerning the flow of phases in the standpipe are outlined next.

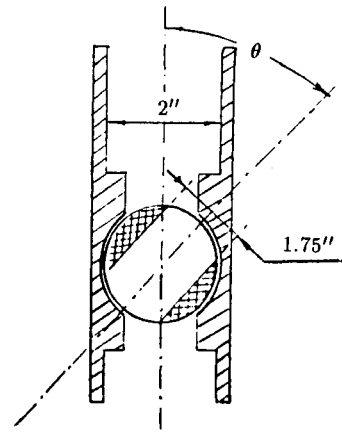


Figure 3. Ball valve.

Li et al. [9] suggested that the mass flow of non-cohesive particles through a valve can be modeled as the flow of solids through an orifice where the Bernoulli relation holds. The particle mass flow in the standpipe can be expressed as:

$$\begin{aligned} \rho_{pm} U_{pm} &= m^* \rho_f U_0 \\ &= C_d (A_o/A) (2\rho_p \alpha_p \Delta P_{op})^{1/2} \\ &= \alpha_p \rho_p W_p, \end{aligned} \quad (4)$$

where C_d is an orifice discharge coefficient; A_o is the area of valve opening which can be varied to give different flow rates of particles; A is the cross-sectional area of the standpipe; α_p is the volume fraction of solids in the standpipe; ΔP_{op} is the pressure drop across the valve; ρ_p is the material density of particles; ρ_{pm} is the mean particle cloud density in pipe flow and U_{pm} is its mean velocity; m^* is the mass flow ratio of particles to fluid measured by the rate of increase of the particle level in the standpipe [1]; ρ_f is density of air of mean velocity U_0 in the pipe. The ball valve is shown schematically in Figure 3. The figure shows the relation A_o/A and angle θ for the adjustment.

When $\alpha_p > 0.2$, [2] proposed an estimation of the particle phase pressure gradient due to gravity in the standpipe with height z_b of solids as:

$$dP_p/dz = \alpha_p \rho_p g = \Delta P_{ps}/z_b, \quad (5)$$

where ΔP_{ps} is the static particle phase pressure drop over the standpipe (or hydrostatic head of particles above the valve). Outside the standpipe, and the ball valve, $P_p \ll P_f$, hence,

$$\Delta P_{op} = \Delta P_{ps}. \quad (6)$$

The above equations give the particle volume fraction as:

$$\alpha_p = m^* U_{op} / C_D (A_o/A) \rho_p (2gz_b)^{1/2}, \quad (7)$$

where C_D is nearly 0.04, calibrated at low solid flow when the volume fraction of solids in the standpipe is nearly that of a packed bed.

For relative motion of phases at low speeds, the inertia forces are negligible. Thus the averaged momentum equation of the fluid phase in the standpipe can be expressed in the form [6]:

$$(1 - \alpha_p) \rho_f F_{fp} (W_p - W_f) - dP_f/dz + (1 - \alpha_p) \rho_f g = 0, \quad (8)$$

with negligible contribution of the Reynolds stress of the fluid phase, where subscript f denotes fluid (air); ΔP_f is the pressure drop in the fluid phase which is measurable; $dP_f/dz = \Delta P_s/z_b$, and axial (z -direction) velocities W is positive in the downward direction; F_{fp} is the relaxation time constant of momentum transfer from particle to fluid. F_{fp} can be determined from the reciprocity relation:

$$(1 - \alpha_p) \rho_f F_{fp} = \alpha_p \rho_p F_{pf}, \quad (9)$$

where the time constant for momentum transfer from fluid to particle, F_{pf} , is given by Equation 3. We note that the gas phase pressure drop as measured by [4] essentially agrees with that given by [7] (Equation 8 without the last term and $W_p = 0$).

Equations 3, 8, and 9 combine to give:

$$(W_p - W_f)[A_2(W_p - W_f) + A_1] = C \equiv (\Delta P_s/z_b) - (1 - \alpha_p) \rho_f g. \quad (10)$$

W_p is given by the last term in Equation 4 and W_f is now given by the quadratic relation

Table 1. Static pressure (Pa) distributions for 100 μ m particles in 51 mm test loop.

m^*, U_o Station	3,10	6,10	9,10	12,10	3,15	6,15	3,8
1	3658	5741	7558	8386	6150	9996	2696
2	2773	3927	4753	6136	5121	7375	2182
8	847	906	1082	1413	1616	1860	593

in Equation 10 as:

$$W_f = W_p - (A_1/2A_2) \{1 - [1 - 4(CA_2/A_1^2)]^{1/2}\}, \quad (11)$$

and a negative value of W_f means an upward leakage flow. Note that Equation 9 reduces to:

$$W_f \cong W_p - (C/A_1), \quad (12)$$

at low velocities. The superficial fluid velocity is now:

$$W_{fs} = W_f(1 - \alpha_p). \quad (13)$$

The above shows that when the column of solid particles in the standpipe is tall enough (large z_b), the air velocity in it could be downward with the solid even at high flow rate of solids. High level of z_b to give large mass flow ratio, however, demands large blower power in the system in Figure 1.

VELOCITIES OF PHASES

The static pressure distributions in the 51 mm diameter test loop were measured by a series of U-tube manometers at points along the loop, as shown in Figure 1. The pressure sensors 1, 2 and 8 were used to estimate the leakage flow through the standpipe. These static pressures for 100 μ m and 450 μ m glass particles with particle mass flow ratios m^* of 3, 6, 9 and 12 at U_o of 10, 15, and 8 m/s were tabulated in Tables 1 and 2. These data were used to estimate the leakage flow through the standpipe, using the relations in the above section. The results

Table 2. Static pressure (Pa) distributions for 450 μm particles in 51 mm test loop.

m^*, U_0	3,10	6,10	9,10	12,10	3,15	6,15	3,8
Station							
1	3820	6282	8364	9888	6826	10498	3797
2	3195	5075	6536	7850	6025	8969	3268
8	913	1157	1420	1554	1960	2355	881

under various test conditions were tabulated in Tables 3 and 4. In each case the superficial air velocity is given by $(1 - \alpha_p)W_f$.

The results indicated that within the range of the experiments, the induced or entrained air flows in the standpipe were small, although there were cases of leakage air flow upward in the standpipe at certain combinations of m^* , U_0 , z_b and particle size. The upward leakage ($W_f < 0$ in Table 4) tends to occur at large solid flow rate, U_0 , and reduced z_b , leading to surging of the solid level, appearance of fluidization bubbles, and a tendency toward the breakdown of continuous feeding of solid particles into the test loop. Stability of the solid flow was also affected by the build-up of static electricity; the latter affects bubble formation [10] in the course of fluidization at large m^* and is affected by the humidity of the air stream and the running time. For instance, at $m^* = 12$ and $U_0 = 10$ and low humidity of air, when air

Table 3. Leakage flows in standpipe for 100 μm particles.

m^*, U_0	3,10	6,10	9,10	12,10	3,15	6,15	3,8
$P_{f3} - P_{f1}$, P_a	2688	4283	5495	6387	4607	7538	2067
A_0/A	0.11	0.24	0.42	0.70	0.17	0.44	0.10
α_p	0.60	0.55	0.50	0.44	0.58	0.48	0.53
z_b , m	1.50	1.45	1.30	1.05	1.50	1.30	1.50
W_p , m/s	0.024	0.052	0.086	0.123	0.039	0.092	0.019
W_f , m/s	0.023	0.050	0.082	0.114	0.038	0.086	0.018

Table 4. Leakage flows in standpipe for 450 μm particles ($W_f < 0$ means upward flow of air).

m^*, U_0	3,10	6,10	9,10	12,10	3,15	6,15	3,8
$P_{f3} - P_{f1}$, P_a	2963	4996	6627	7968	5250	8352	3000
W_p , m/s	0.026	0.058	0.092	0.128	0.043	0.096	0.021
W_f , m/s	0.009	0.015	0	-0.084	0.009	-0.038	-0.008

bubbles appeared in the standpipe, the volume fraction of particles may lower to 0.25 and the interstitial air velocity may reach 0.135 m/s in an upward flow. An arc appeared in the standpipe and the solid level became unstable. Tables 3 and 4 were cases where humidity in the air was maintained above 40%. For details of instrumentation and measurements, refer to [11, 12].

CONCLUSIONS

A standpipe is an important component in the processing and feeding of solid particles. While a large feed rate at small bed height into a flowing stream will lead to instability of solid flow, a tall standpipe for the test loop will call for a large blower power. For a given standpipe, instability of downward flow of solids is not only affected by the flow parameters, but also by the electrostatic charges on particles depending on the humidity of the air stream. For the present test loop system, stability of feed also depends on the pressure drop in the pipe loop.

The present experimental results have illustrated the significance of proper identification of what constitutes pressures of phases. Treating volume fraction of a phase as proportional to its partial pressure is limited to a dilute suspension.

REFERENCES

1. Soo, S.L. "A test facility for pneumatic pipeline design", *Freight Pipelines*, Proc. 6th Int. Freight Pipeline Symp., H. Liu and

- G.F. Round, Eds., Hemisphere Pub. Corp., Washington, DC, pp 209-212 (1990).
2. Chong, Y.O. Teo, C.S. and Leung, L.S. "Recent advances in standpipe flow", *J. Pipelines*, **6**(2), pp 121-132 (1987).
 3. Zhang, Z.Y., Rudolph, V. and Leung, L.S. "Non-fluidized flow of gas-solids in standpipes in under negative pressure gradient", *Fluidization 1989*, Banff, Canada (May, 1989).
 4. Campbell, C.S. and Wang, D.G. "Particle pressures in gas-fluidized beds", *J. Fluid Mechanics*, **227**, pp 495-508 (1991).
 5. Li, H. and Kwauk, M. "Measurement of pressure exerted on the wall by particles in a phase flow", *Engineering Chem. & Metallurgy*, **11**(2), pp 109-113 (in Chinese) (1990).
 6. Soo, S.L. *Particulates and Continuum*, Hemisphere Pub. Co., Washington, DC (1989).
 7. Ergun, S. and Orning, A.A. "Fluid flow through randomly packed columns and fluidized beds", *Ind. Eng. Chem.*, **41**, pp 1179-1184 (1952).
 8. Lin, J.S. "Particle-Tracking Studies for Solids Motion in a Gas Fluidized Bed", Ph.D. thesis, University of Illinois at Urbana Champaign, Urbana, IL 61801 (1981).
 9. Li, X.G., Liu, D.L. and Kwauk, M.S. "Pneumatically controlled multi-state fluidized beds-II", *Proc. Joint Meeting of Chem. Eng., SIESC and AIChE*, Chem. Industry Press, Beijing, pp 382-391 (1982).
 10. Soo, S.L. "Formation of bubbles in a fluidized bed", *J. Powder Tech.*, **10**, pp 211-216 (1974).
 11. Soo, S.L. and Zhu, C. "Unsteady motion of dense suspensions and rheological behavior", *Particulate Two-phase Flow*, M.C. Roco, Ed., Butterworth Publishers, Stoneham, MA (1992).
 12. Zhu, C. "Dynamic Behavior of Unsteady Turbulent Motion Pipe Flows of Dense Gas-Solid Suspensions", Ph.D. thesis, University of Illinois at Urbana-Champaign, Urbana, IL 61801 (August, 1991).

This paper is based on an invited lecture at the memorial session of Professor L.S. Leung of CSIRO, Sydney, Australia, at the ALChE Annual Meeting, Miami, FL, USA, November 3, 1992.